Am J Transl Res 2024;16(7):2840-2851
www.ajtr.org /ISSN:1943-8141/AJTR0156453

Original Article

PTEN-Long inhibits the biological behaviors of glioma cells

Lianting Geng[1*], Zetong Bai[1*], Xichao Wen[1], Haipeng Liu[1], Haipeng Xie[1], Yan Wang[1], Wensong Wu[1], Zhaomu Zeng[2], Kebin Zheng[1]

[1]Department of Neurosurgery, Affiliated Hospital of Hebei University, Baoding 071000, Hebei, China; [2]Department of Neurosurgery, Jiangxi Provincial People's Hospital, The First Affiliated Hospital of Nanchang Medical College, Nanchang 330000, Jiangxi, China. [*]Equal contributors.

Received March 9, 2024; Accepted June 11, 2024; Epub July 15, 2024; Published July 30, 2024

Abstract: Objectives: PTEN-Long is a translational variant of phosphatase and tensin homolog (PTEN). This study aimed to assess the effect of PTEN-Long on the biological characteristics of glioma cells and related mechanisms. Methods: A vector stably expressing PTEN-Long was established and transfected into cells, serving as the overexpression group, while a set of empty vectors served as the negative control group. Real-time reverse transcription-polymerase chain reaction (RT-PCR) and western blot were used to detect the expression of PTEN-Long and phosphatidylinositol 3-kinase, Protein kinase B, andnuclear factor-κB (PI3K-AKT-NF-κB). Cell proliferation was assessed with the Cell Counting Kit 8 (CCK8) assay, migration through the scratch test, and invasion by the transwell chamber assay. Cell cycle analysis was performed using flow cytometry. The volume and weight of subcutaneous tumors in nude mice were also evaluated. Results: PTEN-Long expression led to downregulation of p-Akt, NF-κB p65, p-NF-κB p65, and Bcl-xl, and up-regulation of IκBα. In addition, it inhibited glioma cell proliferation, induced cell cycle arrest in the G0/G1 phase, and reduced cell migration and invasion. Moreover, PTEN-Long inhibited the growth of subcutaneous glioma in nude mice. Conclusions: PTEN-Long inhibits the proliferation, migration, and invasion and induces apoptosis in glioma cells by inhibiting PI3K-AKT-NF-κb signaling, implying that PTEN-Long may be a new target for glioma treatment.

Keywords: Glioma, PTEN-Long, NF-κB p65, proliferation, invasion

Introduction

Gliomas are the most prevalent type of primary intracranial tumor [1]. Despite the availability of treatments such as surgery, radiotherapy, and chemotherapy, the overall survival rate of patients remains very low [2]. Therefore, it is of great significance to investigate the pathogenic mechanism of glioma in depth.

The phosphatase and tensin homologue (PTEN) deleted on chromosome 10 is an important tumor suppressor gene [3-5], and mutations in PTEN are among the most common in solid tumors [6-8]. Two types of PTEN have been identified as translational variants of PTEN, PTEN-Long and PTENα [9, 10]. PTEN-Long, which shares the same phosphatase domain and similar anticancer functions as PTEN, is a secreted protein detectable in human serum and plasma [11]. It exhibits protein phosphatase activities comparable to PTEN [12] and has been found to downregulate p-Akt levels, thereby inhibiting the proliferation of U87 cells [13], replication of HCV [14], growth of renal clear cell tumors [15], and decreasing PINK1-Parkin-mediated mitochondrial autophagy [16]. In addition, several studies have shown that PTEN-Long is reduced in tumor tissues compared to normal tissues. Upregulation of PTEN-Long expression has been reported to inhibit the proliferation of breast cancer and renal cell adenocarcinoma cells and induce tumor regression in murine models of cancer, implying that PTEN-Long may serve as a therapeutic target in cancer [15, 17].

Considering the role of PTEN-Long in several types of solid tumors, whether it plays a role in the pathogenesis and development of gliomas

https://doi.org/10.62347/QHCA5842

Table 1. Sequences of the primers

Primer	Forward: 5'-3'	Reverse: 5'-3'
PTEN-Long	CTCCAAATTTTAAGGTGAAGCTGT	CTCTGGATCAGAGTCAGTGGT
PTEN	CAGAAAGACTTGAAGGCGTAT	AACGGCTGAGGGAACTC
AKT	GCAGCACGTATACGAGAAGA	GGTGTCAGTCTCCGACGTG
NF-κB p65	GAGGACTGCTGCTACGTCAC	ACCAGGTTCAGGTTCAGCTC
IκBα	AACCTGCAGCAGACTCCACT	ACACCAGGTCAGGATTTTGC
bcl-xl	GTAAACTGGGGTCGCATTGT	TGCTGCATTGTTCCCATAGA
β-Actin	CATCCCCCAAAGTTCACAAT	AGTGGGGTGGCTTTTAGGAT

remains unclear. This study therefore evaluated the role and mechanism of PTEN-Long in the biological behavior of glioma cells.

Materials and methods

Cell culture

The U251 human glioma cell line, known for common PTEN mutations and deletions [18], was sourced from the China Infrastructure of Cell Line Resource in Beijing, China. The A172 cell line was obtained from the Cell Bank of the Chinese Academy of Sciences in Shanghai, China. Both cell lines, which exhibit low expression levels of PTEN and PTEN-Long, are well-suited for studies on PTEN-Long. Cells were cultured in Dulbecco's Modified Eagle's Medium (DMEM; Gibco, Grand Island, NY, USA) supplemented with 10% fetal bovine serum (FBS; Gibco) and 1% penicillin-streptomycin, maintained at 37°C in a 5% CO_2 humidified atmosphere.

Cell transfection

To establish cell lines overexpressing PTEN-Long, U251 and A172 cells were seeded into 12-well plates at a density of 1×10^5 cells/well. Upon reaching 70-80% confluency, cells were transfected with LV-PTEN-Long-EGFP. EGFP:T2A:Puro served both as a visual marker and puromycin resistance indicator. EF1A served as the promoter. Mock transfection with LV-EGFP was used as a negative control. The vector was powered by Cyagen Biosciences. Transfection efficiency varied with the multiplicity of infection (MOI) set at 20, 50, and 80. Optimal results were observed at an MOI of 50, where cells maintained good health and exhibited satisfactory EGFP expression levels. Cells were cultured with polybrene (5 μg/ml), and medium was refreshed 6-12 hours post-transfection. Stable clones were selected with puromycin (1.5 μg/ml) for 3-5 days. The transfection efficiency was detected by RT-PCR, western blot, and fluorescence microscopy. The overexpression group was designated as U251-PTEN-Long-EGFP and A172-PTEN-Long-EGFP, and the corresponding negative control groups were U251-EGFP and A172-EGFP. No transfections were performed for the blank control group.

qRT-PCR

Total RNA was extracted from cells using TRIzol reagent (Life Technologies, Rockville, MD, USA) according to the manufacturer's instructions. cDNA synthesis was performed using 1 μg of total RNA with the PrimeScript RT Reagent Kit with gDNA Eraser (Takara, Beijing, China). There was no residual genomic DNA during mRNA preparation. qRT-PCR were carried out with cDNA (1 μl) and SYBR-Green Master Mix (Takara). β-actin served as an internal control. Relative mRNA was quantified using the $2^{-\Delta\Delta Ct}$ method. The sequences of primers are listed in **Table 1**. Additionally, mRNA level was also measured by 1% agarose gel.

Western blotting

Proteins were extracted with cell lysis buffer and separated by SDS-PAGE electrophoresis, followed by transfer to PVDF membranes in an ice bath at constant voltage. The PVDF membranes were incubated with anti-PTEN-Long antibody with gentle rocking at 4°C overnight. The membranes were washed six times with buffer, then incubated with horseradish peroxidase-labeled goat anti-rabbit antibody. ECL illuminating liquid was incubated with the PVDF membranes in the dark. For quantification, bands were analyzed using Image J software. Antibody against PTEN-Long (9188), NF-κB p65 (8242), p-NF-κB p65 (3033), bcl-xl (2764) was purchased from CST, AKT1/2/3

(CY5561), p-Akt (CY6569) were from Abways, IκBα (ab76429) was from Abcam, β-Actin (AF7018) and Goat Anti-Rabbit IgG (H+L) HRP (S0001) was from Affinity.

Cell cycle analysis

Cells were harvested and fixed with pre-cooled 70% ethanol with gentle mixing and stored for 24 h at 4°C. Subsequently, wells were stained with propidium iodide and incubated at 37°C for 30 min in the dark. Red fluorescence was detected at 488 nm by flow cytometry (BD FACSCalibur, US), and the DNA content was analyzed to calculate the percentage of cells in the G1/G0, S, and G2/M phases.

Proliferation assay

U251 and A172 cells were seeded into 96-well plates at a density of 5×10^3 cells/well. CCK-8 reagent (DOJINDO) (10 μl/well) was added after 24, 48, and 72 h post-seeding. After a 3-h incubation, the absorbance at 450 nm was measured with a microplate reader (Bio-Tek EPOCH, US).

Migration analysis

Cells were seeded into 24-well plates at a density of 2×10^5 cells per well with a pore size of 8 μm. Upon reaching 80-90% confluence, the cells were scratched with a sterile tip (200 μl) to form longitudinal cell scratches. After removing the culture medium and washing with PBS twice, the cells were maintained in serum-free medium. Scratched areas were photographed at 0, 12, and 24 h post-wounding using computer-assisted microscopy. The migration was analyzed by measuring the area covered by cell migration.

Invasion assay

Cell invasive ability was detected using Matrigel-coated chambers. 100 μl of Matrigel were added to the upper chamber and incubated at 37°C for 30 min. Cells in FBS-free medium were seeded in the upper chambers (100 μl, 1×10^5) while the lower chamber was filled with medium containing 10% FBS (600 μl). After incubation at 37°C for 24 h, the non-invading cells in upper chamber were wiped with a cotton swab and the lower layer cells were fixed with methanol for 20 min at room temperature. After drying, the cells were dyed in 0.1% crystal violet for 15 min. The chamber was washed with PBS, photographed using a microscope, and the number of invading cells was counted. Five fields were randomly selected for statistical analysis.

Xenograft assays

Twelve BALB/c-nu nude mice (Huafukang, Beijing, China) were randomly divided into 3 groups with 4 mice in each group. U251 cells (100 μl, 5×10^6) were planted subcutaneously on the dorsal side of athymic nude mice and allowed to grow until the tumor reached 1 cm in diameter. A nude mouse subcutaneous tumor model was constructed. The tumor growth was monitored, with the longest (a) and shortest diameters (b) of the tumor were measured with Vernier calipers every 7 days. The tumor volume was calculated using the formula $V = ab^2 \times 0.5$, and a tumor growth curve was plotted. All tumors did not exceed 1.5 cm in diameter, and the weight of the mice did not decrease too much. All mice were included in the study. After 4 weeks, the tumor was removed, weighed, and subjected to immunohistochemical staining. The staining results were analyzed using scoring criteria [19]. Antibodies against PTEN-Long and p-NF-B p65 were purchased from CST, and p-Akt was from Abways. Euthanasia was performed using 100% carbon dioxide at 5 PSI for 3 minutes, followed by a 15-minute waiting period. Death was confirmed by the absence of heartbeat and respiration [12]. The experiment adhered to ethical standards with Animal Ethics Approval No.: 2018015, granted by the Medical Comprehensive Experimental Center of Hebei University.

Statistical analysis

Statistical analyses were conducted using SPSS 19.0. Data are expressed as mean ± SD. Differences between groups were assessed using one-way ANOVA or Repeated measures ANOVA, followed by LSD-t test. Statistical significance was defined as $P<0.05$.

Result

PTEN-Long was stably overexpressed in U251 and A172 cells

PTEN, known for mutations and deletions in a variety of tumors, including gliomas, is closely related to the occurrence and development of

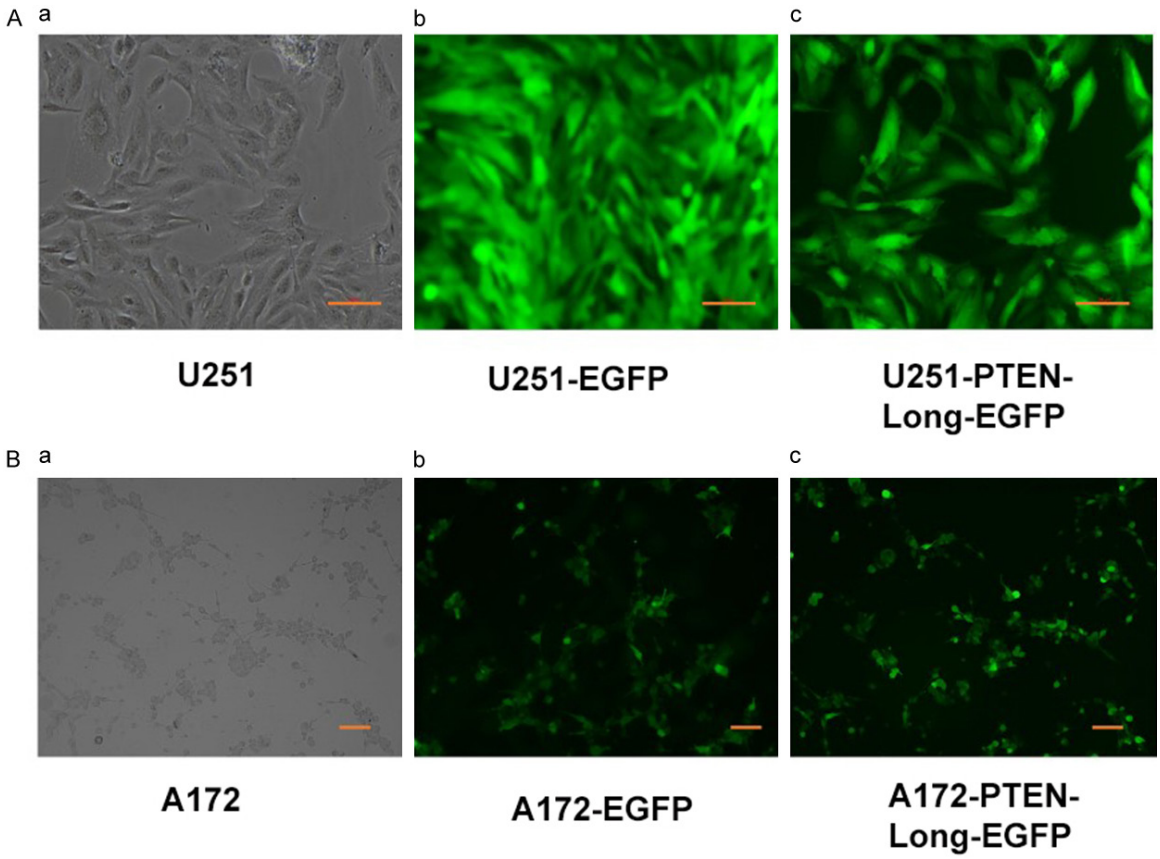

Figure 1. Transfection efficacy analysis. (A, B): (a) Analysis of the EGFP immunofluorescence in U251 and A172 cell lines by a light microscopy; (b) Expression of EGFP in U251 and A172 cells after transfection of LV-EGFP; (c) Expression of PTEN-Long in U251 and A172 cells after transfection of LV-PTEN-Long-EGFP. Bar: 50 μm.

tumors [20]. To explore the antitumor potential of PTEN-Long, a PTEN-Long overexpressing lentiviral vector was constructed. Effective overexpression was achieved with a multiplicity of infection (MOI) of 50, resulting in a fluorescence expression rate exceeding 80%, as observed under a fluorescence microscope (**Figure 1**). Based on RT-PCR and western blot, the expression of PTEN-Long was significantly increased in the overexpression group compared to the control group (P<0.01; **Figures 2**, **3**).

Overexpression of PTEN-Long suppressed PI3K-Akt-NF-κB signaling in U251 cells

In the overexpression group, PTEN-Long was detectable, whereas it was absent in both the negative and blank control groups by western blot analysis. With the increasing in PTEN-Long mRNA and protein levels, the expression of p-Akt, NF-κB p65, p-NF-κB p65, and Bcl-xl in the downstream of PI3K-AKT-NF-κB signal pathway were decreased, while IκBα expression was increased (all P<0.01, **Figures 2**, **3**); However, no significant difference was observed in the expression of AKT and PTEN. Our research showed that PTEN-Long inhibited the activity of PI3K-AKT-NF-κB signal pathway.

Overexpression of PTEN-Long inhibited cell proliferation and blocked the cell cycle

Cell proliferation at different time points was measured using a CCK-8 kit. Compared to negative and blank control groups, cell proliferation activity of the overexpression group decreased from 24 h (all P<0.01; **Figure 4**). Flow cytometry showed that cell cycle was blocked (all P<0.01; **Figure 5**). Our research showed that PTEN-Long suppressed cell proliferation and induced cell apoptosis by blocking cell cycle at G0/G1 phase of glioma cells.

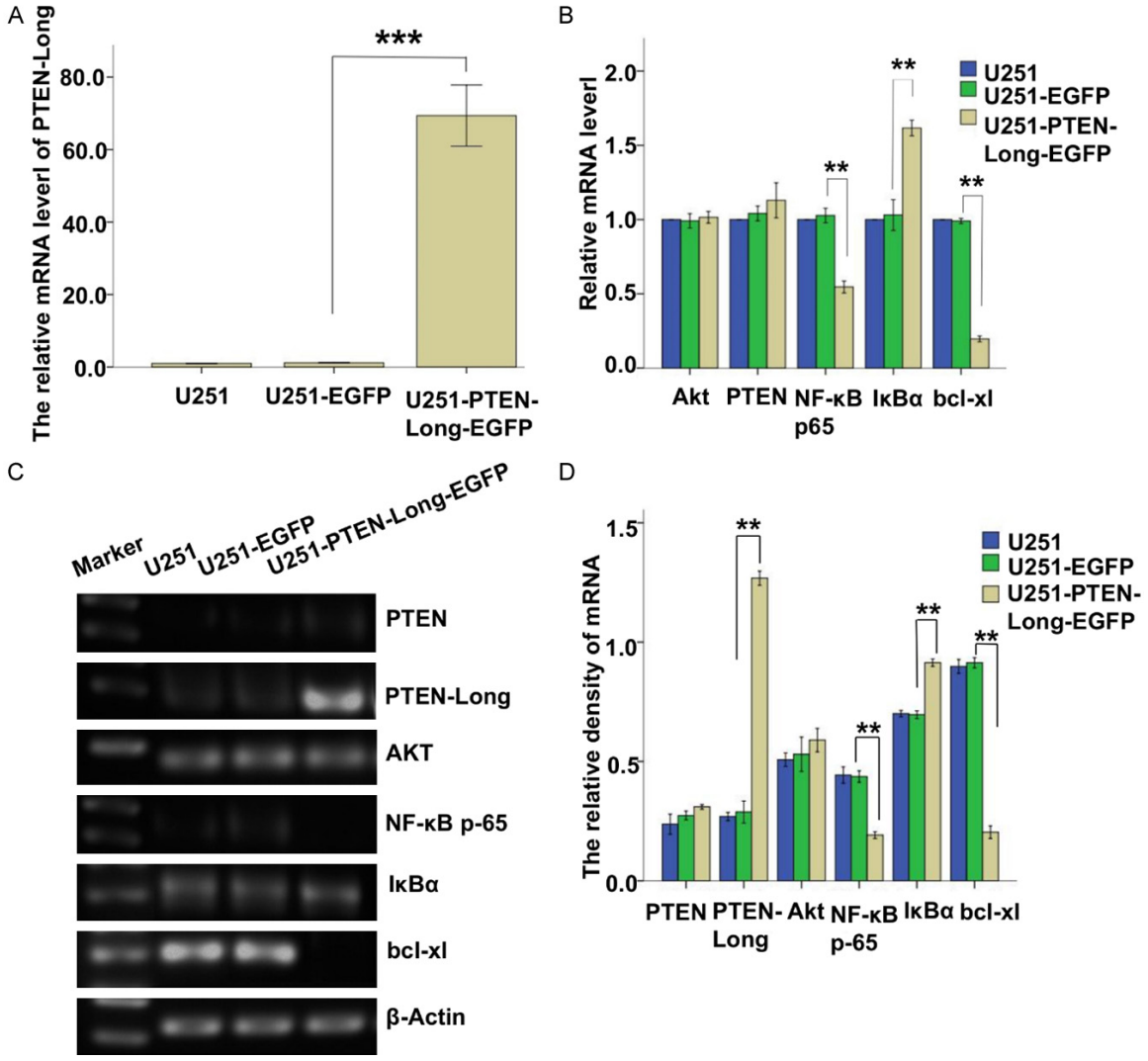

Figure 2. The mRNA level of PTEN-Long, AKT, PTEN, NF-κB p65, IκBa and bcl-xl. A: The quantified results of relative mRNA expression of PTEN-Long. B: The quantified mRNA expression of PI3K-AKT-NF-κB pathway related molecules. C: mRNA expression analyzed by agarose gel electrophoresis after RT-PCR. D: The quantified mRNA expression of PTEN, PTEN-Long, Akt, NF-κb P-65, IκBa and Bcl-xl detected by qRT-PCR. n=3; $^{**}P<0.01$, $^{***}P<0.001$.

Overexpression of PTEN-Long inhibited cell migration and invasion

Scratch test showed that overexpression of PTEN-Long inhibited the migration ability of U251 and A172 cells compared to control groups. Quantitative analysis of the migrated cells 12 and 24 hours post-scratching revealed a significantly larger scratch area in the overexpression group compared to the control group ($P<0.01$; **Figure 6**). Furthermore, the Transwell chamber assay showed that the overexpression of PTEN-Long markedly reduced the invasive ability of glioma cells, with significantly fewer cells invading through the Matrigel compared to the control group ($P<0.01$; **Figure 7**).

PTEN-Long inhibited the proliferation of U251 cells in the xenograft mouse model

We then investigated the function of PTEN-Long on the proliferation of U251 cells in a mouse xenograft model. U251 cells were subcutaneously implanted into athymic nude mice. The tumor growth was monitored every week. By the fourth week, necrosis was observed in the subcutaneous tumor of a mouse in the control group, characterized by tumor bleeding and a deepening color of the subcutaneous tumor. This necrosis was not evident in other tumors. The tumor volume and weight of overexpression group was significantly smaller than those of control group (**Figure 8**). Immunohis-

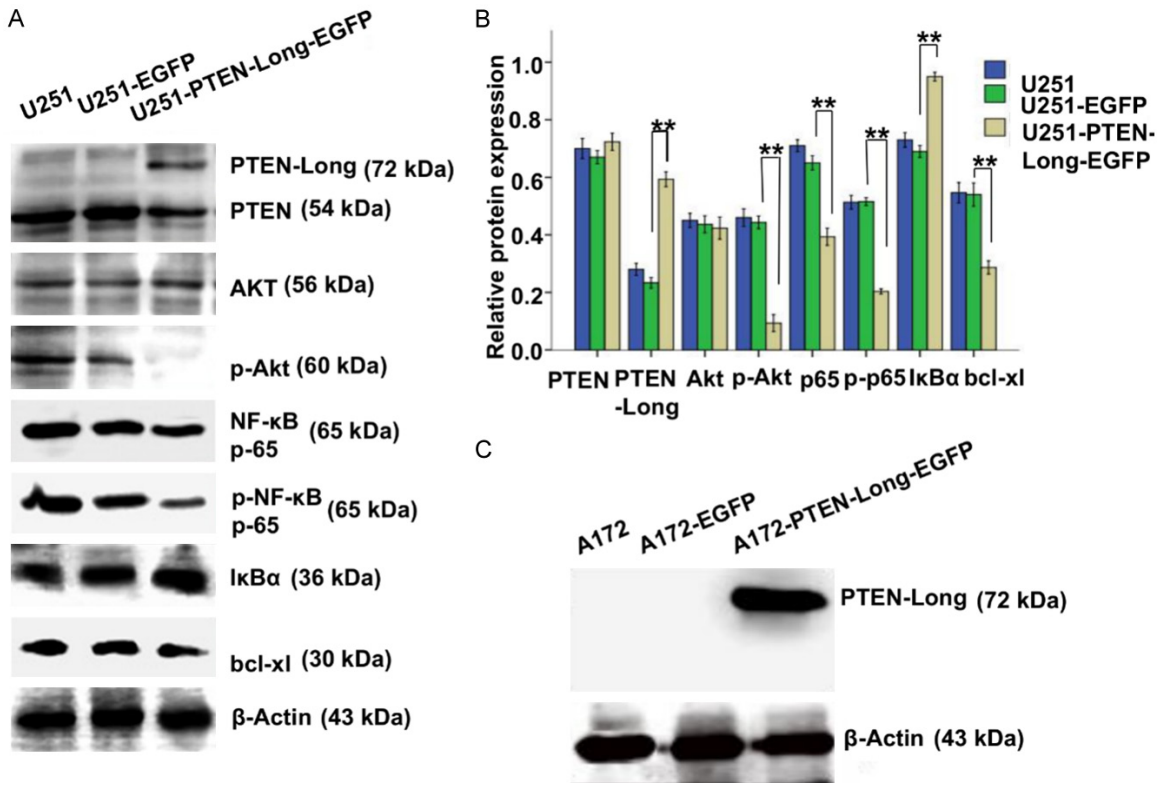

Figure 3. The protein expression of PTEN-Long, AKT, PTEN, NF-κB p65, IκBa and bcl-xl. A: The bands of PI3K-AKT-NF-κB pathway related molecules in each group examined by western blot. B: The normalized relative protein expression of various molecules detected by western blot. C: The expression level of PTEN-Long in each group was examined by western blot. n=3; $^{**}P<0.01$.

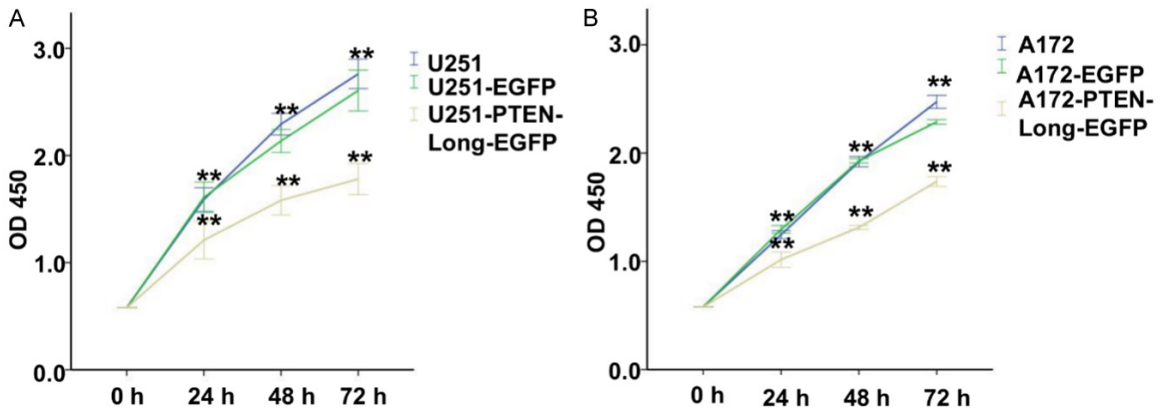

Figure 4. The CCK8 assay was employed to assess cellular viability. The proliferation of U251 cells (A) and A172 cells (B) of each group measured at different points. n=3; $^{**}P<0.01$.

tochemical staining showed a decrease in the expression of p-Akt and NF-κB p65, with a significant decrease in the brown staining in both the cytoplasm and nuclei (**Figure 9**). These results demonstrate that PTEN-Long suppresses cell proliferation by inhibiting the PI3K-Akt-NF-κB signaling pathway, while maintaining tumor burden within recommended limits.

Discussion

Glioma, a prevalent form of intracranial malignancy, has seen a rising incidence, making targeted therapy a critical area of ongoing research. PTEN, an antagonist of PI3K [21-23], inhibits PI3K-AKT and its downstream signal pathway, playing a role in inhibiting tumor cell

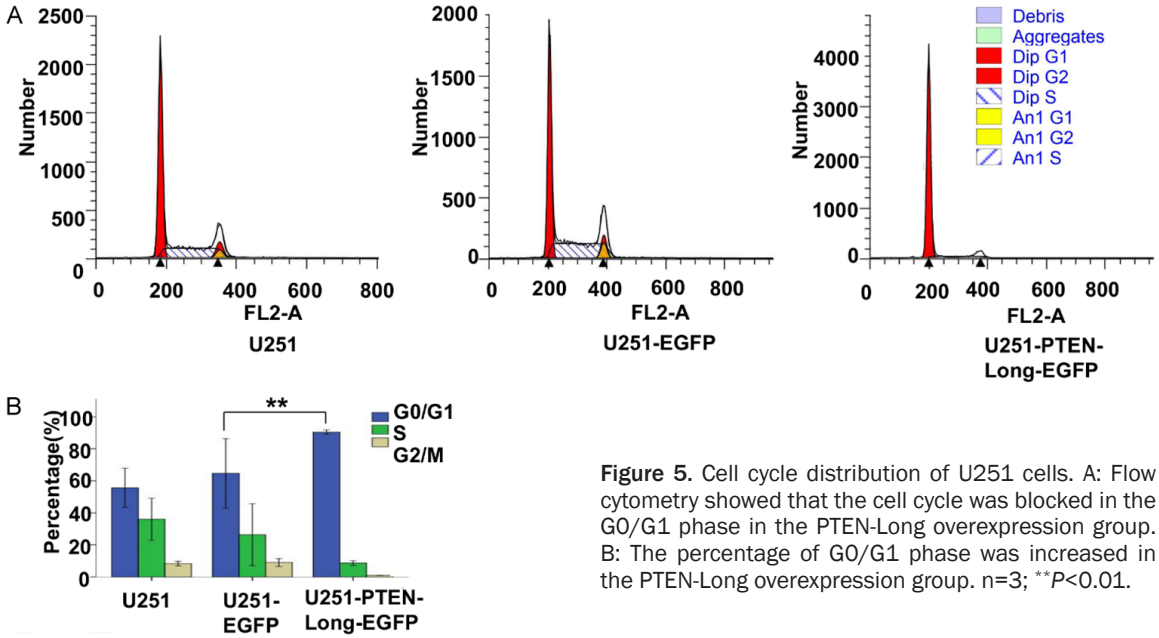

Figure 5. Cell cycle distribution of U251 cells. A: Flow cytometry showed that the cell cycle was blocked in the G0/G1 phase in the PTEN-Long overexpression group. B: The percentage of G0/G1 phase was increased in the PTEN-Long overexpression group. n=3; $^{**}P<0.01$.

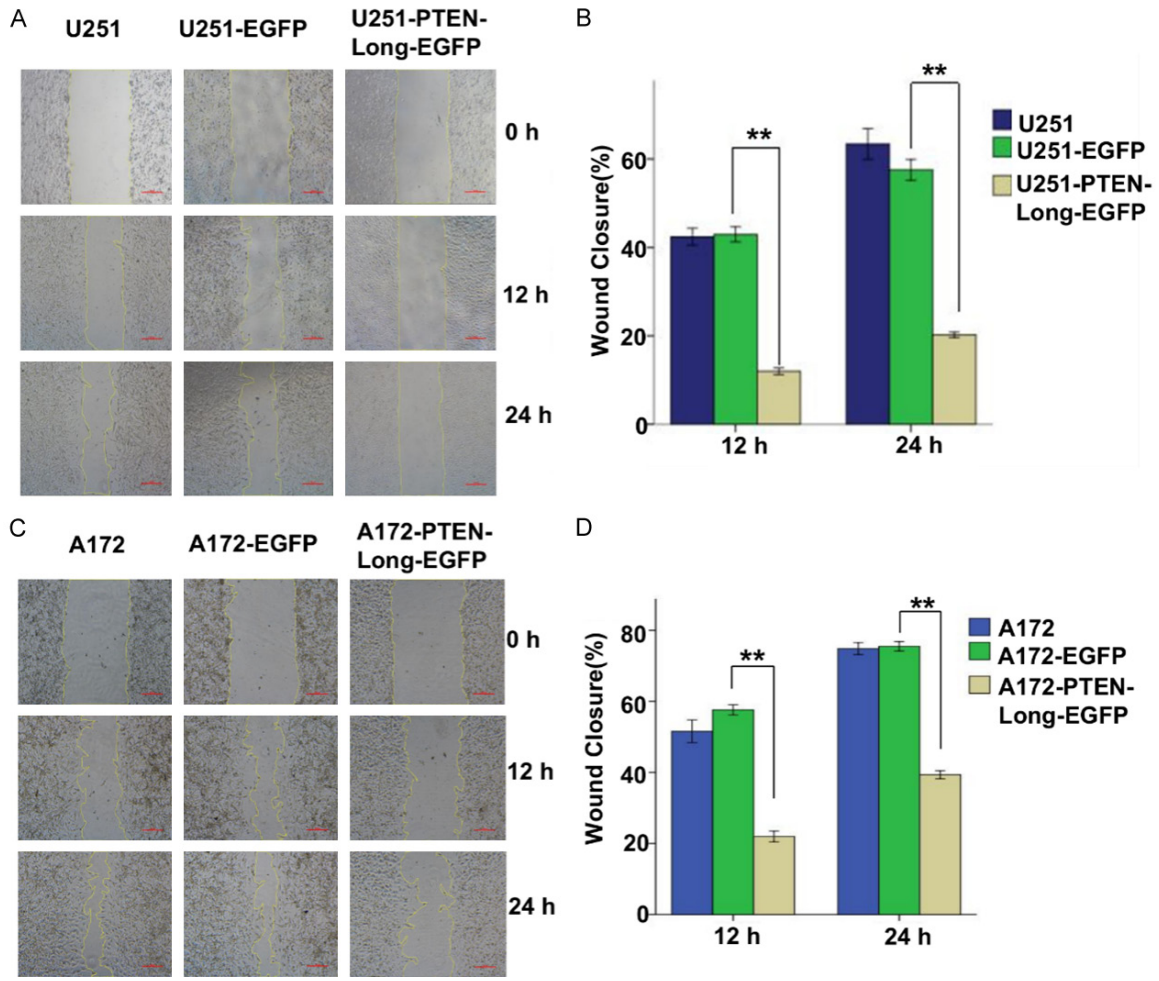

Figure 6. Migration behavior of cells in each group detected by scratch assay. A, B: Migration ability of U251 cells. C, D: Migration ability of A172 cells. SP ×40, Bar: 100 μm; n=3; $^{**}P<0.01$.

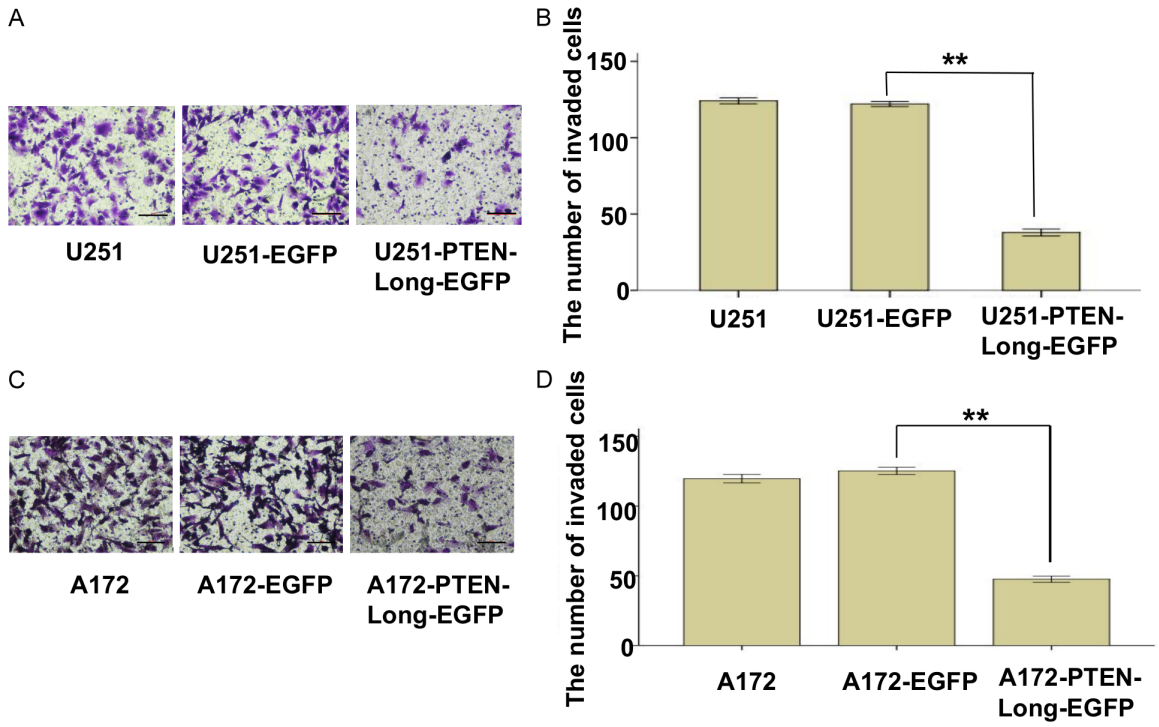

Figure 7. Invasion behavior of cells in each group detected by Transwell assay. A, B: Invasion of U251 cells. C, D: Invasion of A172 cells. SP ×100, Bar: 50 μm; n=3; $^{**}P<0.01$.

proliferation, migration, and invasion, and promoting apoptosis. Studies have shown that it plays a role in many tumor cells, such as BT5-49, U87MG kidney cancer cells, and U251. The protein product of PTEN-Long variant retains the biological activity of PTEN. PTEN-Long can also enter adjacent cells or enter bloodstream, affecting distant cells by a paracrine or endocrine mechanism [24]. The PTEN-Long leader sequence serves as an effective vector for delivering of therapeutic proteins. Specifically, PTEN-L-p53 significantly inhibits the proliferation, migration, and invasion of U251 cells [25].

In U251 and A172 cells, PTEN-Long expression is minimal, as confirmed by qRT-PCR. Due to its low expression, proteins were challenging to detect, and western blot (WB) results indicated similarly low expression levels. This study underscores the value of investigating PTEN-Long expression in PTEN wild-type glioma cells, such as LN-229, which has not been investigated in current research. This study constructed a high expression model of PTEN-Long in U251 and A172 cell lines using lentivirus. Our experiments demonstrated that overexpressing PTEN-Long could suppress proliferation, migration, and invasion of glioma cells. The PI3K-Akt-NF-κB pathway is closely related to these biological properties. Analysis of mRNA and protein expression revealed a decrease in P-Akt, NF-κB p65, and phosphorylated NF-κB p65 in the overexpression group. The underlying mechanism may be that AKT regulates NF-κB activation induced by lipopolysaccharide (LPS). P-Akt activates IKK and NF-κB [26], then the downstream signaling pathway of NF-κB promotes the production of pro-angiogenic factors, which then promotes the production of pro-angiogenic factors, enhancing tumor growth and metastasis [27-29]. PTEN-Long, as the antagonist of PI3K, inhibits Akt phosphorylation, thereby inhibiting PI3K-Akt-NF-κB pathway activity, which includes suppressing nuclear NF-κB p65 activity and decreasing the expression of the anti-apoptotic gene, Bcl-xl. Furthermore, PTEN-Long can block NF-κB activation triggered by tumor necrosis factor-alpha (TNF-α), reduce IκBα degradation, and inhibit Bcl-xl expression, contributing to reduced tumor cell proliferation and apoptosis resistance. However, the absence of direct apoptosis assays in this study is a notable limitation. This study examined the expression of Bcl-xl and analyzed

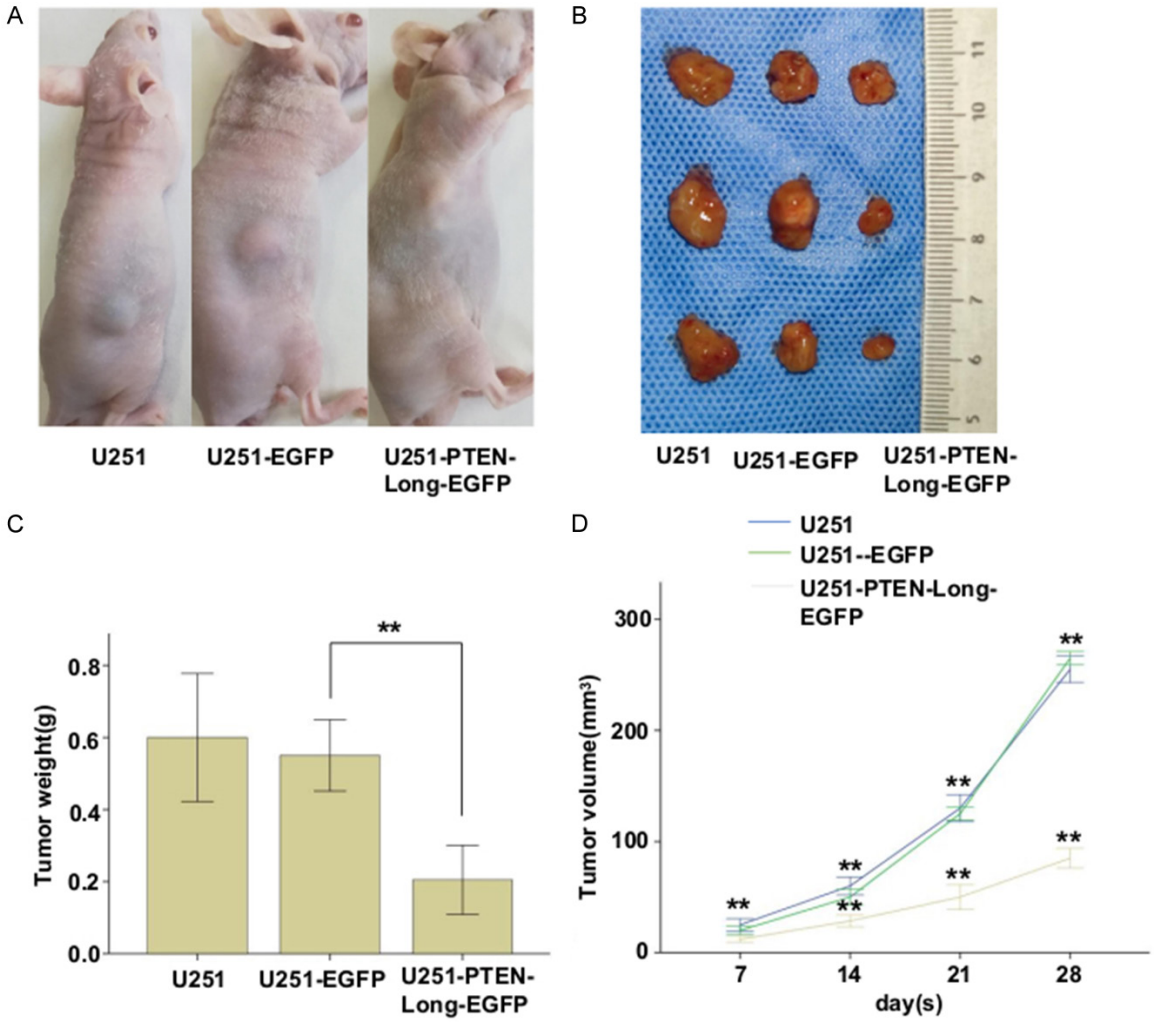

Figure 8. Effect of PTEN-Long on tumor growth *in vivo*. A: Tumor cells were inoculated subcutaneously into nude mice. B: Tumor volume in each group. C: The weight of subcutaneous tumors in each group. D: The Growth curve of subcutaneous tumor volume, measured weekly. **P<0.01.

the possible role of PTEN-Long in cell death, which yielded only a preliminary result. Additionally, Cyclin D1, a target gene of NF-κB that facilitates the G0/G1 to S phase transition and promotes cell proliferation, was examined. PTEN-Long blocks this cell cycle transition, further inhibiting cell proliferation. Animal experiments corroborated that PTEN-Long suppressed glioblastoma proliferation by downregulating the PI3K-Akt-NF-κB signaling pathway, although tumor sizes showed no significant difference between the control group and the empty vector group. This study indicates that PTEN-Long may inhibit glioma through the suppression of the PI3K-Akt-NF-κB signaling pathway. Future research will continue to explore the direct effects of PTEN-Long protein products on glioma cells and the associated molecular mechanisms.

However, gene therapy for glioma faces specific challenges, notably the blood-brain barrier (BBB), which complicates treatment delivery. Research indicates that neural stem cells, owing to their inherent cancer cell homing capabilities, can serve as effective vectors. In our study, replacing the PTEN-Long leader sequence with the human light chain IgG leader sequence addressed issues of drug delivery across the BBB in glioblastoma and improved the intercellular transfer efficiency of the PTEN-Long construct [30]. The use of brain tumor models in nude mice represents a significant step forward, though it also underscores a limi-

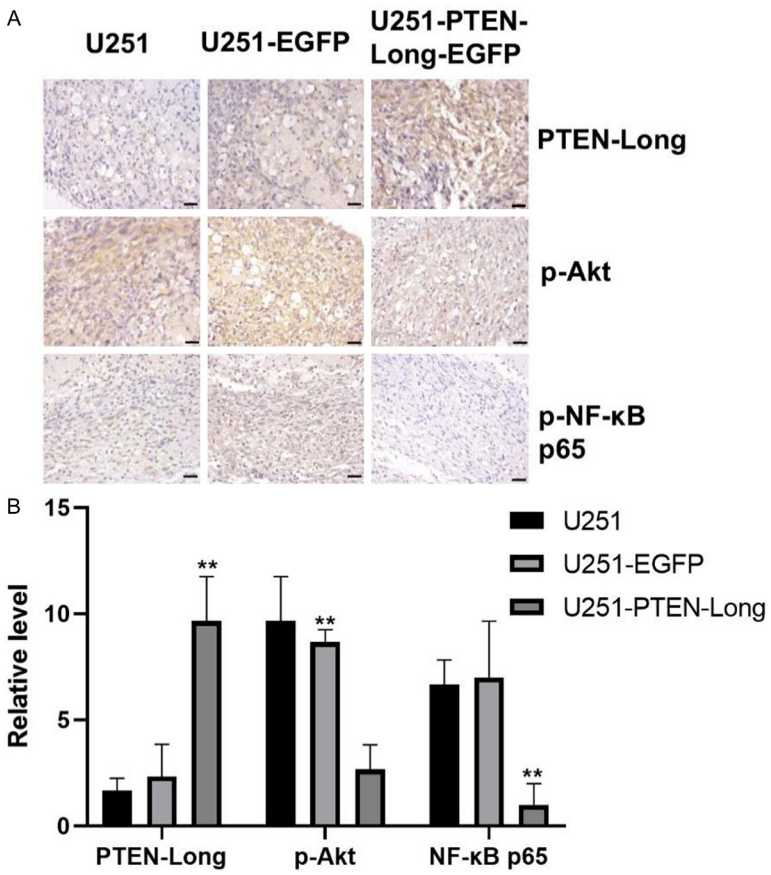

Figure 9. Expression level of PTEN-Long, NF-κB p65, and p-Akt in tumor tissues of each group. A: Immunohistochemical staining. B: Quantification analysis. SP ×400, Bar: 25 μm; n=3; $^{**}P<0.01$.

tation of this study. Therefore, future research should focus on developing a nude mouse brain tumor model to further investigate the therapeutic effects and mechanisms of PTEN-Long on glioma, particularly in the context of the BBB.

In conclusion, the experimental results confirm that PTEN-Long can inhibit the growth of glioma *in vitro* and *in vivo*. PTEN-Long appears to exert its tumor-suppressive effects by downregulating the PI3K-AKT-NF-κB signaling pathway, highlighting its potential as a novel therapeutic target for glioma treatment.

Acknowledgements

Thanks to the Central Laboratory of the Affiliated Hospital of Hebei University and the Medical Comprehensive Experimental Center of Hebei University. This project was supported by the Natural Science Foundation of Hebei Province (No. H2023201032). The funds are used to purchase reagents for performing the experiment.

Disclosure of conflict of interest

None.

Address correspondence to: Zhaomu Zeng, Department of Neurosurgery, Jiangxi Provincial People's Hospital, The First Affiliated Hospital of Nanchang Medical College, No. 266 Fenghe North Avenue, Nanchang 330000, Jiangxi, China. Tel: +86-0791-87721259, E-mail: zzmhemisphere@163.com; Kebin Zheng, Department of Neurosurgery, Affiliated Hospital of Hebei University, No. 212 Yuhua Avenue, Baoding 071000, Hebei, China. Tel: +86-0312-5981818; E-mail: zhengkebin@hbu.edu.cn

References

[1] Stylli SS, Luwor RB, Ware TM, Tan F and Kaye AH. Mouse models of glioma. J Clin Neurosci 2015; 22: 619-626.

[2] Trabelsi S, Brahim DH, Ladib M, Mama N, Harrabi I, Tlili K, Yacoubi MT, Krifa H, Hmissa S, Saad A and Mokni M. Glioma epidemiology in the central Tunisian population: 1993-2012. Asian Pac J Cancer Prev 2014; 15: 8753-8757.

[3] Li J, Yen C, Liaw D, Podsypanina K, Bose S, Wang SI, Puc J, Miliaresis C, Rodgers L, McCombie R, Bigner SH, Giovanella BC, Ittmann M, Tycko B, Hibshoosh H, Wigler MH and Parsons R. PTEN, a putative protein tyrosine phosphatase gene mutated in human brain, breast, and prostate cancer. Science 1997; 275: 1943-1947.

[4] Ray LB. Single-cell biology. Cells go solo. Introduction. Science 2013; 342: 1187.

[5] Wang XR, Luo H, Li HL, Cao L, Wang XF, Yan W, Wang YY, Zhang JX, Jiang T, Kang CS, Liu N and You YP; Chinese Glioma Cooperative Group (CGCG). Overexpressed let-7a inhibits glioma cell malignancy by directly targeting K-ras, independently of PTEN. Neuro Oncol 2013; 15: 1491-1501.

[6] Liaw D, Marsh DJ, Li J, Dahia PL, Wang SI, Zheng Z, Bose S, Call KM, Tsou HC, Peacocke M, Eng C and Parsons R. Germline mutations

of the PTEN gene in Cowden disease, an inherited breast and thyroid cancer syndrome. Nat Genet 1997; 16: 64-67.
[7] Steck PA, Pershouse MA, Jasser SA, Yung WK, Lin H, Ligon AH, Langford LA, Baumgard ML, Hattier T, Davis T, Frye C, Hu R, Swedlund B, Teng DH and Tavtigian SV. Identification of a candidate tumour suppressor gene, MMAC1, at chromosome 10q23.3 that is mutated in multiple advanced cancers. Nat Genet 1997; 15: 356-362.
[8] Yuan TL and Cantley LC. PI3K pathway alterations in cancer: variations on a theme. Oncogene 2008; 27: 5497-5510.
[9] Maehama T and Dixon JE. The tumor suppressor, PTEN/MMAC1, dephosphorylates the lipid second messenger, phosphatidylinositol 3,4,5-trisphosphate. J Biol Chem 1998; 273: 13375-13378.
[10] McGlynn KA, Petrick JL and London WT. Global epidemiology of hepatocellular carcinoma: an emphasis on demographic and regional variability. Clin Liver Dis 2015; 19: 223-38.
[11] Meng X, Lu P and Fan Q. miR-367 promotes proliferation and invasion of hepatocellular carcinoma cells by negatively regulating PTEN (Retraction of Vol 470, Pg 187, 2016). Biochem Biophys Res Commun 2019; 515: 727.
[12] Moriguchi M, Umemura A and Itoh Y. Current status and future prospects of chemotherapy for advanced hepatocellular carcinoma. Clin J Gastroenterol 2016; 9: 184-190.
[13] Fang N, Gu T, Wang Y, Wang S, Wang F, An Y, Wei W, Zhang W, Guo X, Nazarali AJ and Ji S. Expression of PTEN-long mediated by CRISPR/Cas9 can repress U87 cell proliferation. J Cell Mol Med 2017; 21: 3337-3346.
[14] Wu Q, Li Z and Liu Q. Treatment with PTEN-Long protein inhibits hepatitis C virus replication. Virology 2017; 511: 1-8.
[15] Wang H, Zhang P, Lin C, Yu Q, Wu J, Wang L, Cui Y, Wang K, Gao Z and Li H. Relevance and therapeutic possibility of PTEN-Long in renal cell carcinoma. PLoS One 2015; 10: e114250.
[16] Wang LM, Cho YL, Tang YC, Wang JG, Park JE, Wu YJ, Wang CX, Tong Y, Chawla R, Zhang JB, Shi Y, Deng S, Lu G, Wu YH, Tan HWS, Pawijit P, Lim GGY, Chan HY, Zhang JZ, Fang L, Yu H, Liou YC, Karthik M, Bay BH, Lim KL, Sze SK, Yap CT and Shen HM. Author Correction: PTEN-L is a novel protein phosphatase for ubiquitin dephosphorylation to inhibit PINK1-Parkin-mediated mitophagy. Cell Res 2018; 28: 872-873.
[17] Hopkins BD, Fine B, Steinbach N, Dendy M, Rapp Z, Shaw J, Pappas K, Yu JS, Hodakoski C, Mense S, Klein J, Pegno S, Sulis ML, Goldstein H, Amendolara B, Lei L, Maurer M, Bruce J, Canoll P, Hibshoosh H and Parsons R. A secreted PTEN phosphatase that enters cells to alter signaling and survival. Science 2013; 341: 399-402.
[18] Zhang P, Meng X, Liu L, Li S, Li Y, Ali S, Li S, Xiong J, Liu X, Li S, Xia Q and Dong L. Identification of the prognostic signatures of glioma with different PTEN status. Front Oncol 2021; 11: 633357.
[19] van Diest PJ, van Dam P, Henzen-Logmans SC, Berns E, van der Burg ME, Green J and Vergote I. A scoring system for immunohistochemical staining: consensus report of the task force for basic research of the EORTC-GCCG. European Organization for Research and Treatment of Cancer-Gynaecological Cancer Cooperative Group. J Clin Pathol 1997; 50: 801-804.
[20] Han F, Hu R, Yang H, Liu J, Sui J, Xiang X, Wang F, Chu L and Song S. PTEN gene mutations correlate to poor prognosis in glioma patients: a meta-analysis. Onco Targets Ther 2016; 9: 3485-3492.
[21] Cantley LC and Neel BG. New insights into tumor suppression: PTEN suppresses tumor formation by restraining the phosphoinositide 3-kinase/AKT pathway. Proc Natl Acad Sci U S A 1999; 96: 4240-4245.
[22] Maehama T and Dixon JE. The tumor suppressor, PTEN/MMAC1, dephosphorylates the lipid second messenger, phosphatidylinositol 3,4,5-trisphosphate. J Biol Chem 1998; 273: 13375-13378.
[23] Myers MP, Pass I, Batty IH, Van der Kaay J, Stolarov JP, Hemmings BA, Wigler MH, Downes CP and Tonks NK. The lipid phosphatase activity of PTEN is critical for its tumor supressor function. Proc Natl Acad Sci U S A 1998; 95: 13513-13518.
[24] van Ree JH, Nam HJ, Jeganathan KB, Kanakkanthara A and van Deursen JM. Pten regulates spindle pole movement through Dlg1-mediated recruitment of Eg5 to centrosomes. Nat Cell Biol 2016; 18: 814-21.
[25] Xiao M, An Y, Wang F, Yao C, Zhang C, Xin J, Duan Y, Zhao X, Fang N and Ji S. A chimeric protein PTEN-L-p53 enters U251 cells to repress proliferation and invasion. Exp Cell Res 2018; 369: 234-242.
[26] Hou YC, Chiu WC, Yeh CL and Yeh SL. Glutamine modulates lipopolysaccharide-induced activation of NF-κB via the Akt/mTOR pathway in lung epithelial cells. Am J Physiol Lung Cell Mol Physiol 2012; 302: L174-L183.
[27] Jiang H, Zhu YS, Xu H, Sun Y and Li QF. Inflammatory stimulation and hypoxia cooperatively activate HIF-1alpha in bronchial epithelial cells: involvement of PI3K and NF-kappaB. Am J Physiol Lung Cell Mol Physiol 2010; 298: L660-669.
[28] Dilly AK, Ekambaram P, Guo Y, Cai Y, Tucker SC, Fridman R, Kandouz M and Honn KV. Platelet-

type 12-lipoxygenase induces MMP9 expression and cellular invasion via activation of PI3K/Akt/NF-kappaB. Int J Cancer 2013; 133: 1784-1791.

[29] Yen CJ, Izzo JG, Lee DF, Guha S, Wei Y, Wu TT, Chen CT, Kuo HP, Hsu JM, Sun HL, Chou CK, Buttar NS, Wang KK, Huang P, Ajani J and Hung MC. Bile acid exposure up-regulates tuberous sclerosis complex 1/mammalian target of rapamycin pathway in Barrett's-associated esophageal adenocarcinoma. Cancer Res 2008; 68: 2632-2640.

[30] Lavictoire SJ, Gont A, Julian LM, Stanford WL, Vlasschaert C, Gray DA, Jomaa D and Lorimer IAJ. Engineering PTEN-L for cell-mediated delivery. Mol Ther Methods Clin Dev 2017; 9: 12-22.